Available online at www.sciencedirect.com

jmr&t Journal of Materials Research and Technology

journal homepage: www.elsevier.com/locate/jmrt

Original Article

Physicochemical properties and *In vitro* evaluation studies of polyvinylpyrrolidone/cellulose acetate composite nanofibres loaded with *Chromolaena odorata* (L) King extract

Ida Sriyanti [a,b,*], *Leni Marlina* [a], *Ahmad Fudholi* [c,d], *Sherin Marsela* [a], *Jaidan Jauhari* [b]

[a] *Department of Physics Education, Universitas Sriwijaya, Palembang, Indonesia*
[b] *Laboratory of Instrumentation and Nanotechnology Applications, Faculty of Computer Science, Universitas Sriwijaya, Palembang, Indonesia*
[c] *Solar Energy Research Institute, Universiti Kebangsaan Malaysia, 4600, Bangi, Selangor, Malaysia*
[d] *Research Centre for Electrical Power and Mechatronics, Indonesian Institute of Sciences (LIPI), Kawasan LIPI Cisitu, Bandung, Indonesia*

ARTICLE INFO

Article history:
Received 29 December 2020
Accepted 23 February 2021
Available online 3 March 2021

Keywords:
Polyvinylpyrrolidone
Cellulose acetate
Chromolaena odorata
Antibacterial
Antioxidant
Drug release

ABSTRACT

Polyvinylpyrrolidone (PVP)/cellulose acetate (CA) composite nanofibres loaded with *Chromolaena odorata* (L) King extract were prepared using the electrospinning method. The physicochemical properties of nanofibre composites, including their morphology, size, crystallinity, chemical interactions and compressive strength, were studied. *In vitro* tests including antioxidant, antibacterial and release activities were also investigated. The morphology of the nanofibre composites containing *C. odorata* extract (COE) had a smooth, homogeneous and flexible surface and fibres with a diameter of 1454 nm. Fourier-transform infrared spectroscopy analysis showed the interaction of PVP, CA and COE molecules through hydrogen bonds. The XRD pattern showed that crystals were transformed into the amorphous state when COE was converted into nanocomposite fibres. The Young's modulus values of the resulting nanofibre composites were in the range of 199 −209 MPa. The antioxidant activity of PVP/CA nanocomposite fibres contained higher COE than did pure COE, whereas the antibacterial activity of PVP/CA/COE nanofibre was as strong as that of pure COE. The release rate of COE in nanofibres increases faster than does pure COE.

© 2021 The Author(s). Published by Elsevier B.V. This is an open access article under the CC BY-NC-ND license (http://creativecommons.org/licenses/by-nc-nd/4.0/).

* Corresponding author.
E-mail address: ida_sriyanti@unsri.ac.id (I. Sriyanti).

https://doi.org/10.1016/j.jmrt.2021.02.083

2238-7854/© 2021 The Author(s). Published by Elsevier B.V. This is an open access article under the CC BY-NC-ND license (http://creativecommons.org/licenses/by-nc-nd/4.0/).

1. Introduction

Chromolaena odorata (L) King is a tropical plant from the Asteraceae family that is native to African and Asian countries including Malaysia, Thailand and Indonesia [1,2]. In the last decades, this weed has been reported to grow aggressively, particularly in the tropical valleys of Southeast Asia, Africa and the Pacific Islands [3]. This plant can form solid strands in various types of soils that prevent growth and significantly reduce the harvest of cultivated plants such as rubber, coffee, coconut and cashew trees [3]. However, this plant is reported to have many chemical compounds such as tannins, saponins, flavonoids, betacyanins, quinones, glycosides, cardioglycosides, terpenoids, phenols, coumarins, steroids and alkaloids [2,4]. These compounds are reported to have antioxidant [4], antibacterial [5] and anti-inflammatory properties; they also accelerate wound healing [6–10].

A suitable drug delivery technique is required to ensure the utilisation of drug compounds. Electrospinning, a technique to produce thin fibres using high voltage, has introduced new opportunities to develop drug delivery systems. This technique involves the use of Coulombic forces generated by electrical charges to elongate polymer solution forming nanosized polymeric fibres [11–14]. The nanofibre has a small diameter, high porosity and high surface area to mass ratio [14,15]. These characteristics are favourable for biomedical applications such as drug delivery systems [16–19], tissue engineering [20,21] and wound dressings [22–24].

Polyvinylpyrrolidone (PVP) is a non-toxic and biocompatible polymer that has been used for biomedical applications [9]. Previously, PVP has been used as a matrix for the delivery of antibacterial agents such as propolis [10], glycerin and garlic extract [25]. PVP has also been used to deliver antioxidants such as green tea extract and mangosteen pericarp extracts [8,26,27]. PVP is easily degraded upon exposure to high humidity. Thus, it is not suitable for applications in wound dressing [25]. This problem can be overcome by mixing PVP with low aqueous solubility polymers such as cellulose acetate (CA) by electrospinning [28]. CA is a non-toxic polymer that has good biocompatibility, biodegradability and mechanical properties for biomedical applications [29]. In the last few years, several studies reported the application of PVP and CA for drug delivery and a wound dressing matrix. Rachma et al. reported the application of electrospun PVP-Tween 20 for curcumin delivery showing burst release kinetics [30]. The concentration of PVP is proportional to the diameters of the nanofibres. Similar behaviour is also reported for mangosteen delivery [31]. Fast-release kinetics is shown by electrospun PVP/cyclodextrin meloxicam nanofibre mats for oral dosage form [32]. An immediate-release pattern is shown by electrospun PVP/CA fibres containing glycerin and garlic extract [25]. However, few composite nanofibres loaded with *C. odorata* (L) King extract have been developed.

This study intends to synthesise PVP/CA/COE nanofibres by an electrospinning technique. Furthermore, the physicochemical properties of the nanofibre composites will be characterised. The in-vitro antioxidant, antibacterial and release behaviour tests will be also evaluated.

2. Materials and methods

2.1. *Fabrication of PVP/CA composite nanofibres loaded with C. odorata (L) King extract*

PVP with a molecular weight of 1300 kg mol^{-1}, CA with a molecular weight of 500 kg mol^{-1} and 1,1-diphenyl-2-picrylhydrazyl (DPPH) were obtained from Sigma–Aldrich. *C. odorata* (L) King was collected from the South Sumatra forest (Indonesia). Other chemical substances were used without further purification. *C. odorata* (L) King was extracted by maceration using a slightly modified method from the previous experiment [11]. The leaves of CO were cut into smaller pieces and dried in the oven at 40 °C for 2 days. The dried leaves were powdered and macerated in ethanol for 4 days. The extract was then filtered and concentrated using a rotary evaporator (RV 05-ST Janke & Kunkel IKA) at 45 °C and stored properly. CO content in the COE was quantified using UV–Vis spectrophotometry at $\lambda = 201$ nm.

Precursor solutions were made by dissolving each PVP and CA in acetic acid. The solutions of PVP and CA were made at 12 weight%. The PVP and CA solutions were then mixed in the PVP:CA weight ratio of 7:3 and stirred for 4 h. Subsequently, 40 mg of COE was added into 100 mg of a homogenous PVP/CA solution. Nanofibres of PVP/CA and PVP/CA/COE were produced using an electrospinning apparatus (Nanolab, Malaysia). The precursor solution was inserted into a syringe with a 21-gauge needle with an inner diameter of 0.8 cm. During electrospinning, the flow rate of the precursor solutions was maintained at 5 μL/min. The solutions were electrospun at an applied voltage of 10 kV and a gap distance of 12 cm. The temperature and relative humidity used for electospun of nanofibers at 30 ± 1 °C and 60 ± 2%, respectively. The flow chart of fabrication of PVP/CA nanofibre loaded with *C. odorata* (L) King extract is shown in Fig. 1.

2.2. *Characterisations of physicochemical properties composite nanofibre*

The morphology of electrospun fibres of PVP/CA and PVP/CA/COE solutions were characterised by a scanning electron microscope (SEM) (JEOL, JSM-6510). The size distribution of the nanofibres was characterised by Origin 9.0 software. The functional groups and molecular interaction in PVP, CA and COE, as well as PVP/CA/COE were identified by Fourier-transform infrared spectroscopy (FTIR) (Bruker, Alpha). An X-ray diffraction (XRD) pattern of PVP/CA, COE, PVP/CA/COE nanofibre composite were determined using an X-ray diffractometer (Rigaku, SmartLab). The grab and strip test methods are used for the composite nanofibre mats tensile test. Measurements were made using a tensile tester apparatus (Textechno, Favigraph). The extension level and length of the gauge are the same as those previously tested [25]. The maximum tensile strength (UTS) is indicated by the highest

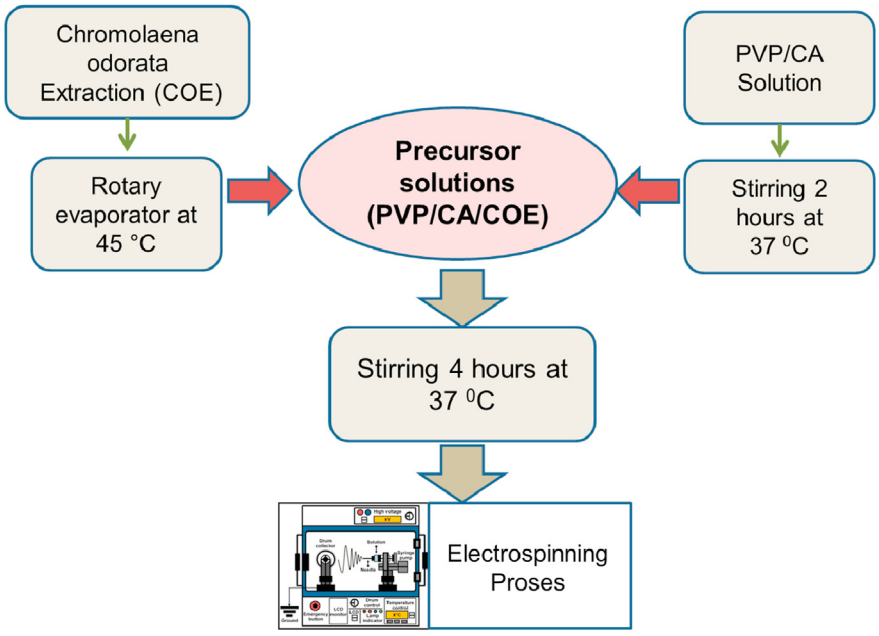

Fig. 1 – Flow chart of fabrication of PVP/CA nanofibre loaded with *C. odorata* (L) King extract.

point of pressure on the curve, and Young's modulus is shown by the comparison of the curve between the highest point of pressure and strain.

2.3. In vitro *antioxidant test*

The antioxidant activity of pure COE and PVP/CA/COE nanofibre was carried out using a modified method reported by Blois with DPPH assay [11,26,33]. This test was carried out *In vitro* to determine whether the electrospinning process with high pressure affects the biological activity of COE. The DPPH test was carried out through antioxidant activity tests on pure COE and COE nanofibre. Various concentrations of pure COE and PVP/CA/COE nanofibre were prepared for this experiment ranging from 10 to 80 μg/mL. Each sample was reacted with the same volume of DPPH solution at a concentration of 50 μg/ml. The mixture was incubated for 30 min. The absorbance of DPPH was measured using a UV–Vis spectrophotometer (Beckman, DU 7500i) at a wavelength of 515 nm. Methanol is used as the blank absorbance. Ascorbic acid is used as a standard ingredient for antioxidant activity. A COE 50 μg/mL DPPH solution was used as a control solution. All samples, namely, pure COE, PVP/CA loaded COE nanofibre and ascorbic acid were analysed in triplicate. The antioxidant activity (% AA) of all samples is determined by the following equation [8,26]:

$$\%AA = \frac{(A_{control} - A_{sampel})}{A_{control}} \times 100 \quad (1)$$

where $A_{control}$ is the absorbance of DPPH in the absence of samples and A_{sample} is the absorbance of DPPH in the presence of samples.

2.4. In vitro *antibacterial test*

The antibacterial activity of the COE and PVP/CA/COE nanofibre were analysed using the disk diffusion method based on the Clinical and Laboratory Standards Institute method [34,35]. The bacterial used was *Staphylococcus aureus* ATCC 6538. The test was started by preparing PVP/CA and PVP/CA/COE composite fibres measuring 3 cm × 3 cm with the same thickness and a masses of 12 and 12.1 mg, respectively. Each PVP/CA/COE and PVP/CA composite fibre was placed on top of Mueller-Hinton Agar (MHA) solids on a Petri dish. An inoculum of *Staphylococcus aureus* bacteria was poured on top of the composite fibre. Then, the test preparations were incubated for 24 h for each sample at 37 °C. After incubation, bacterial colonies were calculated from the dilution to determine the inhibitory activity of bacterial growth using the equation used by previous researchers [25]. Meanwhile, the antibacterial activity of pure COE was tested using the plate count agar test method [36]. A total of 5 mg of pure COE was dissolved in ethanol. The inocula were prepared by mixing 200 μL of the tested bacterial suspension into 20 mL of MHA. Incubation took place at 37 °C for 24 h. To determine the ratio of inhibition to bacterial growth, the following equation [36] is used:

$$Zone\ Inhibition\ (\%) = \frac{C - E}{C} \times 100\% \quad (2)$$

where C is the average number of bacteria in the control sample (without fibres) that grow, and E is the average number of bacteria that grow on the composite fibres after incubation for 24 h.

2.5. In vitro *release*

Pure COE and PVP/CA/COE nanofibre were analysed using a dissolution assay (Hanson Research, SR8 Plus). The method is similar to the previous experiment [11]. The total COE content was determined from the calibration and absorbance curves using a UV–Vis spectrophotometer. The mechanism is carried out by dissolving 40 mg of pure COE or

PVP/CA/COE nanofibre composites that are dispersed in 400 mL of phosphate buffer solution at a physiological pH of 7.4. The mixed solution of the dissolved medium was taken at 5, 10, 15, 30, 45, 60 and 120 min and then replaced with a medium at the same volume. The rotational speed of the oars was 50 rpm and the temperature was maintained at 37 °C, in triplicate. The amount of COE at the stated time interval was measured using a UV–Vis spectrophotometer at a wavelength of 203 nm.

3. Results and discussion

3.1. *Morphology of composite nanofibre*

The surface morphology of the PVP/CA nanofibre with or without COE electron spins is shown in Fig. 2. The morphology of electrospinning results usually appears in the form of fine, beaded, or simple fibres [25]. In this study, the two fibres are in the form of fine fibres, such as hair strands without bead fibres that have a smooth, flexible and homogeneous surface. The presence of COE in PVP/CA fibres does not affect their morphology. This finding is similar to our findings in previous studies in which mangosteen extract did not affect nanofibre formation [11,26]. The size distribution of PVP/CA and PVP/CA/COE fibres is shown in Fig. 2 (a–b). The distribution of the diameter of the PVP/CA fibres is 887 nm with a standard deviation (SD) of 46 nm. The PVP/CA/COE diameter has a size distribution and SD of 1454 and 53 nm, respectively. The addition of COE mass into the PVP/CA composite fibre increases the diameter of the PVP/CA/COE fibre because the addition of COE mass increases the viscosity of the precursors. For precursor solutions with large viscosities, the electric force is difficult to stretch the jet so that the nanofibre diameter generally has a larger diameter [11]. The homogeneity of PVP/CA and PVP/CA/COE fibres was also investigated using the coefficient of variation (CV) of the fibres. The homogeneous curve has a CV of less than 0.3, with a lower CV indicating a greater degree of homogeneity [25]. With CV 0.1, PVP/CA/COE fibres are the more uniform than PVP/CA fibres with CV 0.2.

3.2. *FTIR analysis*

The attenuated total reflectance FTIR spectra of COE, PVP/CA and PVP/CA/COE nanofibres are shown in Fig. 3. The pure FTIR COE spectrum is shown in Fig. 3a. The broad peak at 3373 cm^{-1} indicates O–H stretching (hydroxyl groups). This peak indicates the presence of phenolic compounds [37,38]. This compound acts as an antioxidant from COE or any plant in general. The peak at 1643 cm^{-1} represents the C–O stretching of the carbonyl and carboxylate groups, while the peak at a medium intensity at 1423 cm^{-1} shows N–H bending. This peak is formed due to flexible vibrations of O–H in carboxylic acids, which indicate the presence of flavonoids, tannins,

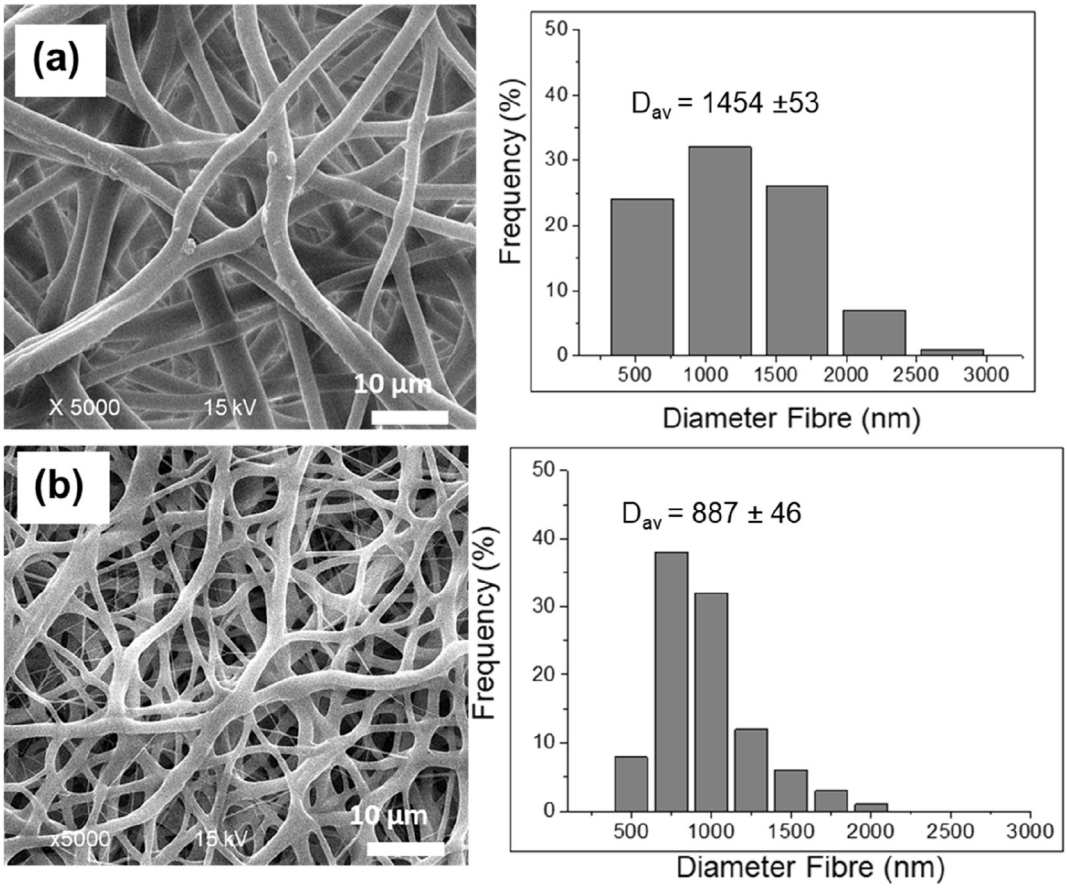

Fig. 2 – SEM image of (a) PVP/CA fibre and (b) PVP/CA/COE fibre.

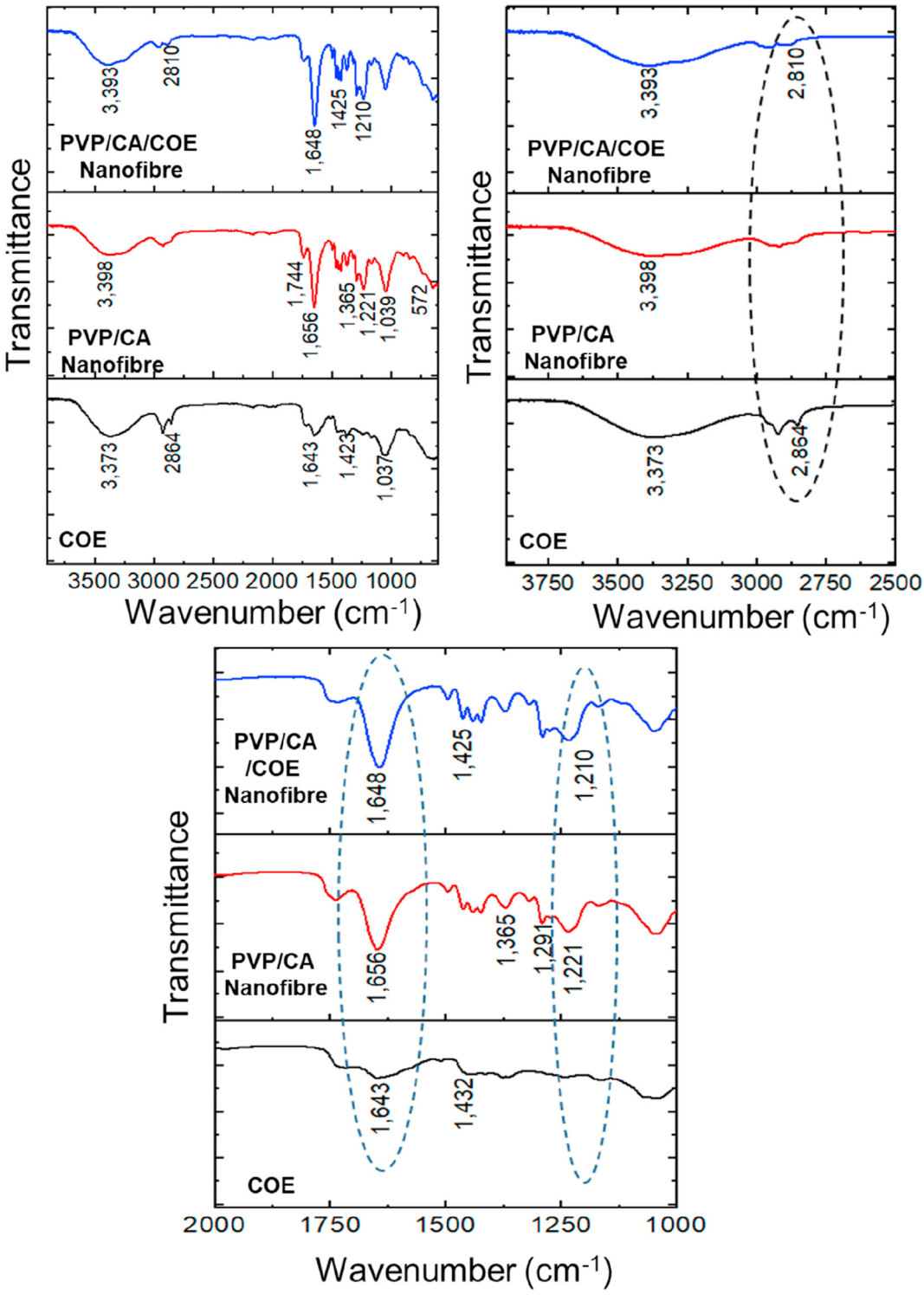

Fig. 3 – FTIR spectra of COE, PVA/CA nanofibre, and PVA/CA/COE nanofibre.

saponins and glycosides [25]. Tannins, saponins and glycosides are known to act as an antibacterial activity for COE. By contrast, the peak at 1037 showed C–N stretching [37]. The peaks at 2864 cm-1 was assigned to symmetric CH2 stretching [19].

The PVP/CA FTIR spectrum is shown in Fig. 3b. The presence of the PVP molecule is characterised by a sharp peak at 1656 cm^{-1} indicating C=O stretching of the cyclic amide group. Meanwhile, the peaks at 1291 and 572 cm^{-1} indicate C–N stretching and in-plane N–C=O. The CA FTIR spectrum has a sharp peak at 1744 cm^{-1}, which is the stretching of the C=O (acetyl group). The peak at 1365 cm^{-1} shows C–H vibrations. The peaks at 1221 and 1039 cm^{-1} are characteristic of the carboxyl acid groups [39,40]. The addition of COE in the

PVP/CA fibre resulted in several changes in the peaks of the PVP/CA/ODE nanofibre waves as shown in Fig. 3c, namely (1) the intensity of the peak band 3800–3000 cm^{-1} (O–H stretching), which negated the presence of phenolic compounds getting sharper. A band intensity at 1500–1400 cm^{-1} (N–H bending) indicated antibacterial properties. (2) New peaks with a small band intensity formed at 2950 cm^{-1}. (3) The addition of COE causes the typical peak of PVP to shift to a low wavenumber from 1653 to 1648 cm^{-1} as well as the typical peak of carboxyl acid to switch from 1234 to 1230 cm^{-1}. Changes in intensity, the formation of new peaks, and peak shifts in wavenumbers for FTIR spectroscopy occur because the COE was well included in the PVP/CA nanofibre.

3.3. *XRD analysis*

The XRD patterns of pure COE, PVP/CA nanofibre and PVP/CA/COE nanofibre composites are shown in Fig. 4. The typical diffraction pattern of pure COE (Fig. 4a) has six sharp diffraction peaks between angles of 2θ positions 5°–80° of 13.9°, 16.64°, 25.31°, 28.22°, 40.34° and 73.54°. These peaks indicate the crystalline nature of COE. By contrast, the PVP/CA fibres (Fig. 4b) present a broad halo pattern in which four weak diffraction peaks occur between the angles of 2θ at the 5°–30° positions, namely 23.1°, 33.3°, 36.8° and 49.32°. The 23° peak represents the PVP, and the 36° peak is the typical CA peak [41]. This broad peak indicates that the diffraction pattern of the PVP/CA nanofibre molecules is amorphous. This finding is consistent with those of Jauhari et al. (2019) that the diffraction pattern of PVP and CA is amorphous [41].

The XRD pattern of COE in PVP/CA/COE shows the crystal transformation to the amorphous state. PVP/CA dispersed dramatically in the prepared sample and caused a decrease in the degree of crystallinity of the COE. In our study, conversion to the amorphous state was most likely to occur during electrospinning. The applied voltage causes the polymer solution to rapidly move from the tip of the needle to the collector. At the same time, the polymer undergoes elongation along with solvent evaporation, resulting in solidification into fibres. In this very short time, the PVP, CA and COE molecules are unable to rearrange their three-dimensional structure. As a result, the molecules are not arranged so highly that they are at the crystal level. This finding is consistent with those of Rahma et al. [30] stated that the electrospinning process delayed the crystallization of polymers, and this corresponded with our results.

Fig. 4 depicts the X-ray diffraction spectra for the PVP/CA/COE nanofibre composite. The addition of COE in the PVP/CA nanofibre produced a new pattern, namely, a broad halo with three peaks at 2θ of 16.32°, 21.44° and 25.3°. The three peaks show representative peaks of COE, PVP and CA recorded in the peaks of the PVP/CA/COE composite fibre. Typical peaks of COE are seen at 2θ of 16.32°, PVP peaks are shown at 21.44° angles and CA peaks at 2θ of 25.3°. The presence of typical COE, PVP and CA patterns in PVP/CA/COE nanofibres shows that COE, PVP and CA molecules form interactions between molecules through hydrogen bonds. These findings reinforce the analysis of the FTIR study that we previously described.

3.4. *Tensile properties of the composite nanofibre*

The mechanical properties of wound dressing materials are considered important because they require certain tensile strength properties and Young's modulus (MPa) for handling and replacement. The ultimate tensile properties and Young's

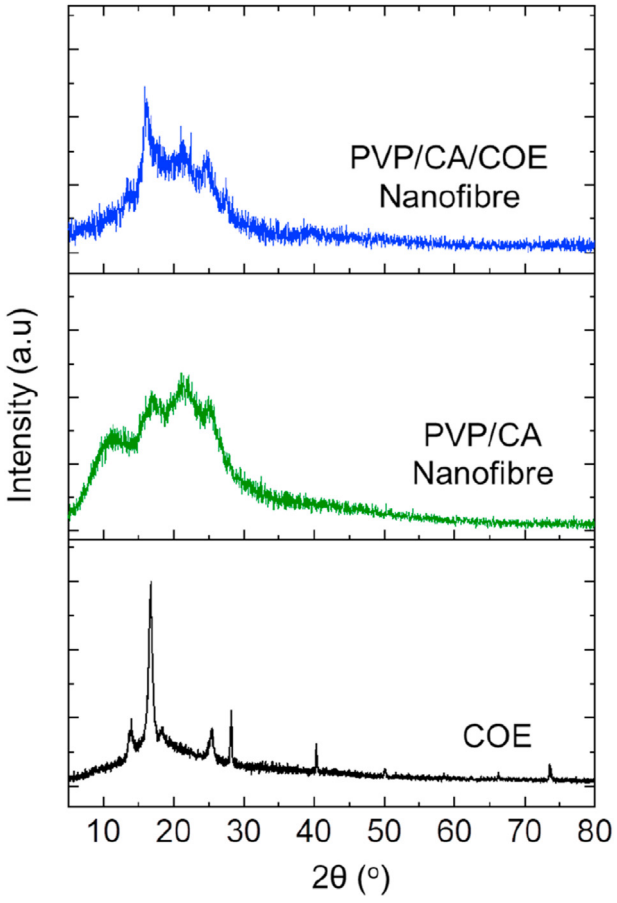

Fig. 4 – XRD of COE, PVP/CA nanofibre, and PVP/CA/COE nanofibre.

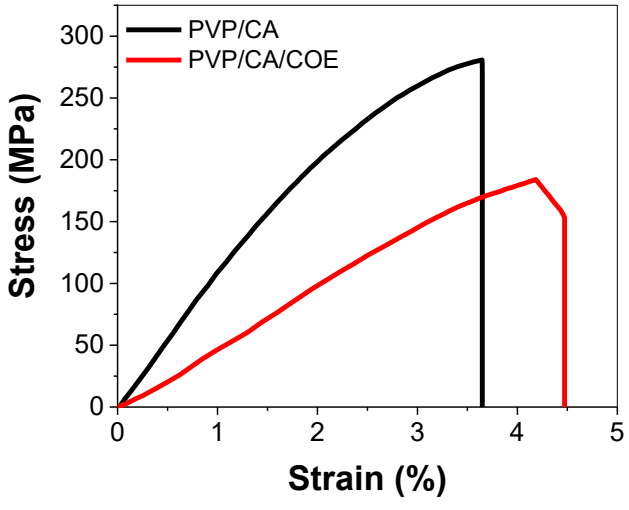

Fig. 5 – Graphs describing the relation between pressure and strain for all fibrous mats.

Table 1 – Young's modulus and ultimate tensile strength for PVP/CA and PVP/CA/COE.

Samples	Diameter (nm)	Ultimate tensile strength (MPa)	Young's modulus (MPa)
PVP/CA	887	7.654 ± 0.12	209.77 ± 0.32
PVP/CA/COE nanofiber	1454	5.01 ± 0.15	119.7 ± 0.34

modulus of the composite are shown in Fig. 5 and Table 1. The addition of COE in PVP/CA fibres reduces the tensile strength and Young's modulus, showing that the fibre is less flexible. The reason for this finding is that fibres with a larger diameter have lower tensile strength and elongation and vice versa. This finding is related to the degree of molecular orientation of the polymer chains in the fibre. At a given polymer mass, fibres with a larger diameter have fewer polymer chains, whereas fibres with a smaller diameter have more polymer chains oriented parallel to each other; thus, more bonds are formed between the chains [41,42]. Furthermore, the decrease in tensile strength of PVP/CA/COE nanofibres is due to amorphous conditions. The Young's modulus values of the two nanofibres produced were in the range 119–209 MPa, which was above the Young's modulus limit required for wound dressing (a minimum of 20 MPa).

3.5. *Antioxidant activity of the composite fibre and COE*

COE extract contains 40 beneficial flavonoid compounds capable of eradicating free radicals present at the wound site. Therefore, COE can clean dead cells and reduce the wound healing period [43]. The antioxidant properties of COE nanofibres were studied by the DPPH assay. The colour of the DPPH solution changed from purple to yellow after incubation with COE, showing a cooling of DPPH free radicals by flavonoid groups in pure COE and COE nanofibres, thereby forming stable compounds. The antioxidant activity of pure COE and PVP/CA/COE fibre is explained by the IC_{50} value. The antioxidant activity of pure COE and PVP/CA/COE fibre is explained by the IC50 value. The antioxidant activity of the compounds is very high in the range of 1–50 μg/mL. In the high category, the value is between 50 and 100 ug/mL; in the moderate category, the value is within 101–150 ug/mL; and in the weak category, the value is greater than 150 ug/mL [26,44]. Table 2 shows that the IC_{50} value of ascorbic acid (reference) has the same high antioxidant activity as did PVP/CA/COE nanofibre and pure COE. Meanwhile, the two samples tested obtained higher PVP/CA/COE nanofibre antioxidant activity values (IC_{50}) than did COE. The effect of the very high surface properties of the nanofibre makes the flavonoid compounds of COE release at a certain time so that it can extinguish free radicals from outside more effectively than can pure COE. These results indicate that the stability of biologically active compounds in COE can still be maintained during electrospinning. In previous studies, we have reported that the antioxidant activity of polyvinylpyrrolidone nanofibre containing GME is superior to that of GME without nanofibre [11]. The effect of the surface area of the nanofibres also resulted in the antioxidant activity of polycaprolactone–chlorophenol nanofibres equivalent to that of *C. phlomidis* leaf extract [45].

Table 2 – Antioxidant activities of ascorbic acid, COE and PVP/CA/COE nanofibre.

Sample	Diameter (nm)	IC_{50} (μg/mL)	Antioxidant activity
Ascorbic acid	–	2.28 ± 0.17	Very high
COE	–	24.88 ± 0.26	Very High
PVP/CA/COE nanofiber	1454	16.81 ± 0.31	Very High

3.6. *Antibacterial activity of the composite fibre and COE*

The antibacterial test results for PVP/CA/COE and PVP/CA fibres showed that the inhibition zone for PVP/CA/COE and PVP/CA fibres against *Staphylococcus aureus* did not appear. The reason for this finding may be the same as that described by Dhewa et al. (2019) that the effect of circular-cut fibres with a size of 3 cm × 3 cm causes a low COE mass in the fibre to be insufficient be important to antibacterial activity [25]. Therefore, carrying out further activities is necessary to ascertain whether the PVP/CA/COE and PVP/CA fibres have antibacterial activity. The total count plate technique was used by taking agar from PVP/CA/COE and PVP/CA fibre and wiping it onto an MHA, then incubating for another 24 h. After incubation, bacterial colonies for control and all mats were observed. The number of bacterial colonies of PVP/CA/COE composite fibre, PVP/CA composite fibre and control are 1.05 × 1,010, 1.38 × 1012 and 1.90 × 1012 cfu/mL, respectively. The ability to inhibit the growth of PVP/CA/COE bacteria was higher than the PVP/CA and control fibres. The reason for this result is the smaller number of bacterial colonies than the PVP/CA fibres and the control. The results showed that the PVP/CA/COE composite fibre has the potential for antibacterial activity. The alkaloid and tannin compounds found in COE affect the ability to inhibit *Staphylococcus aureus* bacteria [5].

The pure COE antibacterial test was performed using the total plate technique. A total of 5 mg COE was diluted in ethanol with concentrations of 1,000, 100, 50, 25 and 10 μg/mL. An inhibition zone diameter (cm) COE against *Staphylococcus aureus* is formed, where the inhibition zone image is shown in Fig. 6 and the inhibition zone pure COE diameter is 17.1 ± 0.23 mm. According to Bate et al. [34], samples with an inhibition area of ≥20 mm are classified into the high active category. If the area of resistance is 10–20 mm, then it is classified into the moderately active category [34]; if the area is less than 10 mm, it is characterised into the weak category [46]. The results indicate that pure COE is included in the moderate category of inhibiting *Staphylococcus aureus* bacteria. The results showed that COE had the potential for antibacterial activity.

3.7. In vitro *release of the composite fibre (PVP/CA/COE) and COE*

Study releases are an important aspect of the drug release system. The pure COE release and the PVP/CA/COE nanofibre are shown in Fig. 7. In general, the release of COE in nanofibre has two phases of release. The first release phase is preceded by a burst release, which is characterised by a large amount of

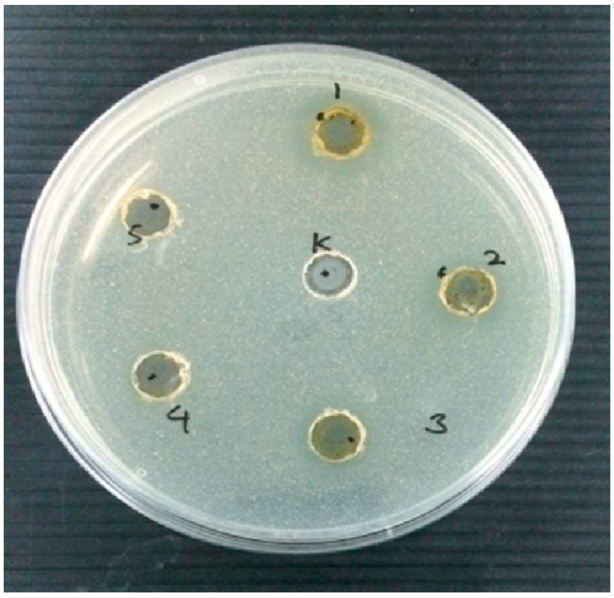

Fig. 6 – Images of the zones of inhibition of COE.

COE released in a very short time with a cumulative average of 35% at 5 min. The rapid release is influenced by (1) the attractive properties of the nanofibres, that is, the ratio of surface area to volume of large nanofibres dramatically increases the rate of drug release and a larger surface area, thereby leading to an increase in the total fraction of drug released [47,48]. (2) XRD studies show that the structure of the PVP/CA/COE nanofibre is amorphous. In this state, the amorphous molecular interactions are weaker than the crystalline conditions [49]. Previous research shows that the amorphous phase of PLGA fibres may increase solubility because the increased surface area enables the N-acetylcysteine to be wet by solvent easily [50]. Consequently, PVP/CA/COE nanofibres tend to diffuse into the release medium at high speed compared with pure COE. However, the mean cumulative COE released from the nanofibres is lower than that in our previous study [11], perhaps influenced by the CA polymer in the nanofibre that has low solubility. The second phase is the release of COE slowly reaching 80% in 120 min. At this stage, the nanofibres begin to degrade because they are dissolved in the solution of the medium along with the release of the COE that is incorporated in the fibre; the rate of release of COE into the medium solution begins to slow down to its maximum release. These results agree with those by Rahma [30] that the release of active substances from nanofibres can occur by diffusion or erosion/degradation. The time required to achieve mass erosion makes the rate of release slower than that in the previous phase [51].

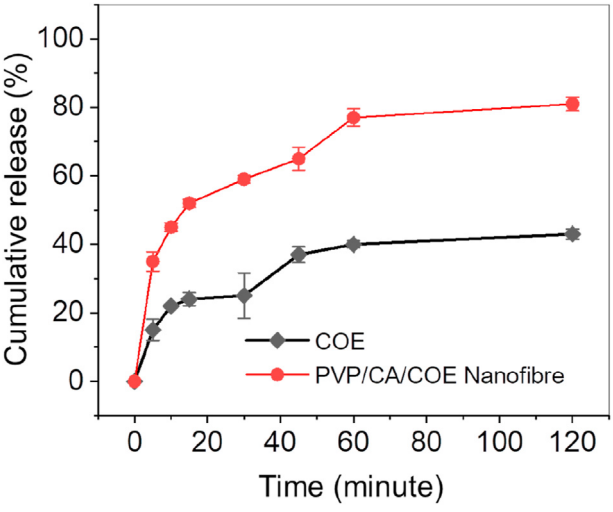

Fig. 7 – Release profile of PVP/CA/COE and COE.

4. Conclusions

The electrospinning technique is used to make PVP/CA fibres containing COE. SEM analysis shows that the fibre size increases with the inclusion of COE into the nanofibre. The FTIR findings indicate the formation of hydrogen O–H stretching, which indicates the presence of phenolic compounds, and N–H bending, which indicates antibacterial compounds in the PVP/CA/COE nanofibres. The XRD pattern of the fibre shows an amorphous pattern. The Young's modulus values of the two nanofibres produced were in the range of 119–209 MPa, where values that were above the Young's modulus limit were required for wound dressings. *In vitro* antioxidants showed that PVP/CA/COE nanofibres performed radical scavenging, which was as effective as pure COE and could inhibit *Staphylococcus aureus* bacteria. The electrospinning process using high voltage exposure did not affect the antioxidant and antibacterial activity of nanofibres. The release of COE from nanofibres is faster than that of pure COE. This speed is facilitated by the high surface area of the nanofibre network. The high antioxidant and the increased release rate of nanofibres gives PVP/CA/COE the potential to increase the yield offered by COE. These findings suggest that the nanocomposite fibre mat can be applied in the pharmaceutical industry as a potential antioxidant and antibacterial product.

Declaration of Competing Interest

The authors declare that they have no known competing financial interests or personal relationships that could have appeared to influence the work reported in this paper.

Acknowledgements

This research was financially supported by Universitas Sriwijaya, Republik of Indonesia, under the University's Excellence Research (PUPT) Grant for the fiscal year of 2020–2021.

REFERENCES

[1] Buhyan M, Deb P, Dasgupta D. Chromolaena odorata: as nature's wound healer. Int J Curr Pharmaceut Res 2019:63–5. https://doi.org/10.22159/ijcpr.2019v11i4.34955.

[2] Omokhua AG, McGaw LJ, Chukwujekwu JC, Finnie JF, Van Staden J. A comparison of the antimicrobial activity and *In vitro* toxicity of a medicinally useful biotype of invasive *Chromolaena odorata* (Asteraceae) with a biotype not used in traditional medicine. South Afr J Bot 2017;108:200–8. https://doi.org/10.1016/j.sajb.2016.10.017.
[3] Rofida S, Nurwahdaniati. Antibacterial activity of Chromolaena odorata (L) King leaves with bioautography. Pharmacy 2015;12:29–36.
[4] Bhargava D, Mondal C, Shivapuri J, Mondal S, Kar S. Antioxidant properties of the leaves of *Chromolaena odorata* linn. J Inst Med 2013;35. https://doi.org/10.3126/joim.v35i1.8900.
[5] Nanadini N, Nagababu P, Umamaheswara Rao V, Venugopal N. Phytochemical, antimicrobial and antioxidant properties of an invasive weed-*Chromolaena odorata* (L.) King & Robinson. Int J Phytomed 2014;6:286–92.
[6] Sirinthipaporn A, Jiraungkoorskul W. Wound healing property review of siam weed, chromolaena odorata. Pharm Rev 2017;11:35–8. https://doi.org/10.4103/phrev.phrev_53_16.
[7] Aruan NM, Sriyanti I, Edikresnha D, Suciati T, Munir MM, Khairurrijal K. Polyvinyl alcohol/soursop leaves extract composite nanofibers synthesized using electrospinning technique and their potential as antibacterial wound dressing. Procedia Eng 2017;170:31–5. https://doi.org/10.1016/j.proeng.2017.03.006.
[8] Pusporini P, Edikresnha D, Sriyanti I, Suciati T, Munir MM, Khairurrijal K. Electrospun polyvinylpyrrolidone (PVP)/green tea extract composite nanofiber mats and their antioxidant activities. Mater Res Express 2018;5. https://doi.org/10.1088/2053-1591/aac1e6.
[9] Dai X-Y, Nie W, Wang Y-C, Shen Y, Li Y, Gan S-J. Electrospun emodin polyvinylpyrrolidone blended nanofibrous membrane: a novel medicated biomaterial for drug delivery and accelerated wound healing. J Mater Sci Mater Med 2012;23:2709–16. https://doi.org/10.1007/s10856-012-4728-x.
[10] Asawahame C, Sutjarittangtham K, Eitssayeam S, Tragoolpua Y, Sirithunyalug B, Sirithunyalug J. Antibacterial activity and inhibition of adherence of Streptococcus mutans by propolis electrospun fibers. AAPS PharmSciTech 2014;16:182–91. https://doi.org/10.1208/s12249-014-0209-5.
[11] Sriyanti I, Edikresnha D, Rahma A, Munir MM, Rachmawati H, Khairurrijal K. Mangosteen pericarp extract embedded in electrospun PVP nanofiber mats: physicochemical properties and release mechanism of α-mangostin. Int J Nanomed 2018;13:4927–41. https://doi.org/10.2147/IJN.S167670.
[12] Ramakrishna S, Fujihara K, Teo W-E, Lim T-C, Ma Z. An introduction to electrospinning and nanofibers. An introd to electrospinning nanofibers. 2010. https://doi.org/10.1142/9789812567611.
[13] Alarifi IM, Khan WS, Asmatulu R. Synthesis of electrospun polyacrylonitrile-derived carbon fibers and comparison of properties with bulk form. PloS One 2018;13. https://doi.org/10.1371/journal.pone.0201345.
[14] Kusumah FH, Sriyanti I, Edikresnha D, Munir MM, Khairurrijal. Simply electrospun gelatin/cellulose acetate nanofibers and their physico-chemical characteristics. Mater Sci Forum 2016;880:95–8. https://doi.org/10.4028/www.scientific.net/MSF.880.95.
[15] Elsayed MT, Hassan AA, Abdelaal SA, Taher MM, khalaf Ahmed M, Shoueir KR. Morphological, antibacterial, and cell attachment of cellulose acetate nanofibers containing modified hydroxyapatite for wound healing utilizations. J Mater Res Technol 2020;9:13927–36. https://doi.org/10.1016/j.jmrt.2020.09.094.
[16] Sakuldao S, Yoovidhya T, Wongsasulak S. Coaxial electrospinning and sustained release properties of gelatin-cellulose acetate core-shell ultrafine fibres. Sci Asia 2011;37:335–43. https://doi.org/10.2306/scienceasia1513-1874.2011.37.335.
[17] Gupta KC, Haider A, Choi YR, Kang IK. Nanofibrous scaffolds in biomedical applications. Biomater Res 2014;18. https://doi.org/10.1186/2055-7124-18-5.
[18] Wang C, Ma C, Wu Z, Liang H, Yan P, Song J, et al. Enhanced bioavailability and anticancer effect of curcumin-loaded electrospun nanofiber: *in vitro* and *in vivo* study. Nanoscale Res Lett 2015;10:1–10. https://doi.org/10.1186/s11671-015-1146-2.
[19] Rahma A, Munir MM, Khairurrijal, Rachmawati H. The influence of non-ionic surfactant on the physical characteristics of curcumin-loaded nanofiber manufactured by electrospinning method. Adv Mater Res 2015;1112:429–32. https://doi.org/10.4028/www.scientific.net/AMR.1112.429.
[20] Vasita R, Katti DS. Nanofibers and their applications in tissue engineering. Int J Nanomed 2006;1:15–30. https://doi.org/10.2147/nano.2006.1.1.15.
[21] Liu H, Ding X, Zhou G, Li P, Wei X, Fan Y. Electrospinning of nanofibers for tissue engineering applications. J Nanomater 2013;2013. https://doi.org/10.1155/2013/495708.
[22] Rasekh M, Karavasili C, Soong YL, Bouropoulos N, Morris M, Armitage D, et al. Electrospun PVP–indomethacin constituents for transdermal dressings and drug delivery devices. Int J Pharm 2014;473:95–104. https://doi.org/10.1016/j.ijpharm.2014.06.059.
[23] Liu X, Lin T, Gao Y, Xu Z, Huang C, Yao G, et al. Antimicrobial electrospun nanofibers of cellulose acetate and polyester urethane composite for wound dressing. J Biomed Mater Res B Appl Biomater 2012;100B:1556–65. https://doi.org/10.1002/jbm.b.32724.
[24] Charernsriwilaiwat N, Rojanarata T, Ngawhirunpat T, Sukma M, Opanasopit P. Electrospun chitosan-based nanofiber mats loaded with Garcinia mangostana extracts. Int J Pharm 2013;452:333–43. https://doi.org/10.1016/j.ijpharm.2013.05.012.
[25] Edikresnha D, Suciati T, Munir MM, Khairurrijal K. Polyvinylpyrrolidone/cellulose acetate electrospun composite nanofibres loaded by glycerine and garlic extract with *In vitro* antibacterial activity and release behaviour test. RSC Adv 2019;9:26351–63. https://doi.org/10.1039/C9RA04072B.
[26] Sriyanti I, Edikresnha D, Rahma A, Munir MM, Rachmawati H, Khairurrijal K. Correlation between structures and antioxidant activities of polyvinylpyrrolidone/Garcinia mangostana L. Extract composite nanofiber mats prepared using electrospinning. J Nanomater 2017;2017:1–10. https://doi.org/10.1155/2017/9687896.
[27] Andjani D, Sriyanti I, Fauzi A, Edikresnha D, Munir MM, Rachmawati H, et al. Rotary forcespun polyvinylpyrrolidone (PVP) fibers as a mangosteen pericarp extracts carrier. Procedia Eng 2017;170:14–8. https://doi.org/10.1016/j.proeng.2017.03.003.
[28] Tungprapa S, Puangparn T, Weerasombut M, Jangchud I, Fakum P, Semongkhol S, et al. Electrospun cellulose acetate fibers: effect of solvent system on morphology and fiber diameter. Cellulose 2007;14:563–75. https://doi.org/10.1007/s10570-007-9113-4.
[29] Wu C-S. Mechanical properties, biocompatibility, and biodegradation of cross-linked cellulose acetate-reinforced polyester composites. Carbohydr Polym 2014;105:41–8. https://doi.org/10.1016/j.carbpol.2014.01.062.
[30] Rahma A, Munir MM, Khairurrijal, Prasetyo A, Suendo V, Rachmawati H. Intermolecular interactions and the release pattern of electrospun curcumin-polyvinyl(pyrrolidone)

fiber. Biol Pharm Bull 2016;39:163–73. https://doi.org/10.1248/bpb.b15-00391.
[31] Sriyanti I, Edikresnha D, Munir MM, Rachmawati H, Khairurrijal. Electrospun polyvinylpyrrolidone (PVP) nanofiber mats loaded by Garcinia mangostana L. Extracts. Mater Sci Forum 2017;880:11–4. https://doi.org/10.4028/www.scientific.net/MSF.880.11.
[32] Samprasit W, Akkaramongkolporn P, Ngawhirunpat T, Rojanarata T, Kaomongkolgit R, Opanasopit P. Fast releasing oral electrospun PVP/CD nanofiber mats of taste-masked meloxicam. Int J Pharm 2015;487:213–22. https://doi.org/10.1016/j.ijpharm.2015.04.044.
[33] Blois MS. Antioxidant determinations by the use of a stable free radical. Nature 1958;181:1199–200. https://doi.org/10.1038/1811199a0.
[34] Bate PNN, Orock AE, Nyongbela KD, Babiaka SB, Kukwah A, Ngemenya MN. *In vitro* activity against multi-drug resistant bacteria and cytotoxicity of lichens collected from Mount Cameroon. J King Saud Univ Sci 2020;32:614–9. https://doi.org/10.1016/j.jksus.2018.09.001.
[35] Tatah AJ-F, Ngunde PJ, Evelyn MS, Gerard N, Ndip RN. Risk factors for wound infection in health care facilities in Buea, Cameroon: aerobic bacterial pathogens and antibiogram of isolates. Pan Afr Med J 2014;18. https://doi.org/10.11604/pamj.2014.18.6.2304.
[36] Moussa SH, Tayel AA, Al-Hassan AA, Farouk A. Tetrazolium/formazan test as an efficient method to determine fungal chitosan antimicrobial activity. J Mycol 2013;2013:1–7. https://doi.org/10.1155/2013/753692.
[37] Alara OR, Abdurahman NH. GC–MS and FTIR analyses of oils from Hibiscus sabdariffa, Stigma maydis and Chromolaena odorata leaf obtained from Malaysia: potential sources of fatty acids. Chem Data Collect 2019;20:100200. https://doi.org/10.1016/j.cdc.2019.100200.
[38] Duygu D, Udoh A, Ozer T, Akbulut A, Erkaya I, Yildiz K, et al. Fourier transform infrared (FTIR) spectroscopy for identification of Chlorella vulgaris Beijerinck 1890 and Scenedesmus obliquus (Turpin) Kützing 1833. Afr J Biotechnol 2012;11. https://doi.org/10.5897/AJB11.1863.
[39] Kiatyongchai T, Wongsasulak S, Yoovidhya T. Coaxial electrospinning and release characteristics of cellulose acetate-gelatin blend encapsulating a model drug. J Appl Polym Sci 2014;131. https://doi.org/10.1002/app.40167. n/a-n/a.
[40] Baganizi DR, Nyairo E, Duncan SA, Singh SR, Dennis VA. Interleukin-10 conjugation to carboxylated PVP-coated silver nanoparticles for improved stability and therapeutic efficacy. Nanomaterials 2017;7. https://doi.org/10.3390/nano7070165.
[41] Jauhari J, Wiranata S, Rahma A, Nawawi Z, Sriyanti I. Polyvinylpyrrolidone/cellulose acetate nanofibers synthesized using electrospinning method and their characteristics. Mater Res Express 2019;6:064002. https://doi.org/10.1088/2053-1591/ab0b11.
[42] Yao J, Bastiaansen CWM, Peijs T. High strength and high modulus electrospun nanofibers. Fibers 2014;2:158–87. https://doi.org/10.3390/fib2020158.
[43] Putri DA, Fatmawati S. A new flavanone as a potent antioxidant isolated from chromolaena odorata L. Leaves. Evid Based Compl Altern Med 2019;2019. https://doi.org/10.1155/2019/1453612.
[44] Fidrianny I, Natalia S, Insanu M. Antioxidant capacities of various fruit extracts from three varieties of tomato and correlation with total phenolic, flavonoid, carotenoid content. Int J Pharm Clin Res 2015;7:283–9.
[45] Khoshnevisan K, Maleki H, Samadian H, Doostan M, Khorramizadeh MR. Antibacterial and antioxidant assessment of cellulose acetate/polycaprolactone nanofibrous mats impregnated with propolis. Int J Biol Macromol 2019;140:1260–8. https://doi.org/10.1016/j.ijbiomac.2019.08.207.
[46] Dhivya C, Vandarkuzhali SAA, Radha N. Antimicrobial activities of nanostructured polyanilines doped with aromatic nitro compounds. Arab J Chem 2019;12:3785–98. https://doi.org/10.1016/j.arabjc.2015.12.005.
[47] Pillay V, Dott C, Choonara YE, Tyagi C, Tomar L, Kumar P, et al. A review of the effect of processing variables on the fabrication of electrospun nanofibers for drug delivery applications. J Nanomater 2013;2013. https://doi.org/10.1155/2013/789289.
[48] Dhand C, Dwivedi N, Sriram H, Bairagi S, Rana D, Lakshminarayanan R, et al. 8 - nanofiber composites in drug delivery. In: Ramalingam M, editor. Ramakrishna SBT-NC for BA. Woodhead Publishing; 2017. p. 199–223.
[49] Meng F, Trivino A, Prasad D, Chauhan H. Investigation and correlation of drug polymer miscibility and molecular interactions by various approaches for the preparation of amorphous solid dispersions. Eur J Pharmaceut Sci 2015;71:12–24. https://doi.org/10.1016/j.ejps.2015.02.003.
[50] Mahumane GD, Kumar P, Pillay V, Choonara YE. Repositioning N-acetylcysteine (NAC): NAC-loaded electrospun drug delivery scaffolding for potential neural tissue engineering application. Pharm Times 2020;12. https://doi.org/10.3390/pharmaceutics12100934.
[51] Fu Y, Kao WJ. Drug release kinetics and transport mechanisms of non-degradable and degradable polymeric delivery systems. Expet Opin Drug Deliv 2010;7:429–44. https://doi.org/10.1517/17425241003602259.